Virology 488 (2016) 216–224

Contents lists available at ScienceDirect

Virology

journal homepage: www.elsevier.com/locate/yviro

Rabies virus phosphoprotein interacts with ribosomal protein L9 and affects rabies virus replication

Youwen Li [a,b,d,1], Wanyu Dong [a,b,1], Yuejun Shi [a,b], Feng Deng [a,b], Xi Chen [a,b], Chunyun Wan [b], Ming Zhou [a,b], Ling Zhao [a,b], Zhen F. Fu [a,b,c,*], Guiqing Peng [a,b,**]

[a] The National Key Laboratory of Agricultural Microbiology, Huazhong Agricultural University, Wuhan, Hubei 430070, China
[b] College of Veterinary Medicine, Huazhong Agricultural University, Wuhan, Hubei 430070, China
[c] Departments of Pathology, College of Veterinary Medicine, University of Georgia, Athens, GA 30602, USA
[d] College of Animal Science, Tarim University, Alar, Xinjiang, China

ARTICLE INFO

Article history:
Received 7 June 2015
Returned to author for revisions
9 November 2015
Accepted 19 November 2015
Available online 4 December 2015

Keywords:
Rabies virus
Ribosomal protein L9
Protein interaction
Viral replication and transcription

ABSTRACT

Rabies virus is a highly neurotropic virus that can cause fatal infection of the central nervous system in warm-blooded animals. The RABV phosphoprotein (P), an essential cofactor of the virus RNA-dependent RNA polymerase, is required for virus replication. In this study, the ribosomal protein L9, which has functions in protein translation, is identified as P-interacting cellular factor using phage display analysis. Direct binding between the L9 and P was confirmed by protein pull-down and co-immunoprecipitation analyses. It was further demonstrated that L9 translocates from the nucleus to the cytoplasm, where it colocalizes with P in cells infected with RABV or transfected with P gene. RABV replication was reduced with L9 overexpression and enhanced with L9 knockdown. Thus, we propose that during RABV infection, P binds to L9 that translocates from the nucleus to the cytoplasm, inhibiting the initial stage of RABV transcription.

Introduction

Rabies, caused by rabies virus (RABV), remains a global public health problem with approximately 59,000 human deaths annually (McCarthy, 2015). RABV, a member of the family Rhabdoviridae, is a non-segmented negative-strand RNA virus. (Ray et al., 1995). The genome of RABV encodes five viral proteins, including the nucleoprotein (N), phosphoprotein (P), matrix protein (M), glycoprotein (G), and large RNA-dependent RNA polymerase (L or RdRp) (Jackson, 2002). The N, P, and L of RABV participate in viral transcription and replication in a regulated and efficient manner (Fu et al., 1994; Mavrakis et al., 2006).

P is a phosphorylated protein and consists of 297 amino acid residues (Chenik et al., 1998). P is a nonenzymatic cofactor that associates with the polymerase L and interacts with N to aid viral replication (Chenik et al., 1994; Fu et al., 1994; Jacob et al., 2001). The major L-binding site locates in the N-terminal 19 residues of P (Chenik et al., 1998). P contains two N protein-binding domains: one domain in the C-terminus (residues 268–297) binds to N-RNA, and the other (residues 69–139) binds to N° (not bound to viral RNA) (Chenik et al., 1994; Mavrakis et al., 2003, 2004).

P is also considered to be the primary interferon (IFN) antagonist because of its capacity to bind signal transducer and activator of transcription (STAT) proteins, which causes the nuclear exclusion of the P-STAT complex via a strong export sequence within P (Mavrakis et al., 2004; Pasdeloup et al., 2005; Vidy et al., 2005; Wiltzer et al., 2014). In addition, P can interact with the cytoplasmic dynein light chain (LC8), which is involved in the retrograde axonal transport of RABV (Raux et al., 2000). RABV is attenuated by simultaneously modifying the dynein light chain binding site in P and replacing Arg333 in the glycoprotein (Mebatsion, 2001). The P-LC8 interaction is not involved in viral spread but in primary viral transcription (Tan et al., 2007).

The ribosomal protein L9 (rpL9 or L9) is a 192-amino-acid protein and one of the ribosomal large subunit proteins (Wool et al., 1995). L9 is essential for the translational function of the ribosome and plays an important role in proper ribosome formation (Beyer et al., 2013) . In addition, L9 can interact with the mouse mammary tumor virus (MMTV) Gag protein in cells

* Corresponding author at: Department of Pathology, College of Veterinary Medicine, University of Georgia, 501 D.W. Brooks Drive, Athens, GA 30602, USA. Fax: +1 706 542 5828.
** Corresponding author at: State-key Laboratory of Agricultural Microbiology, College of Veterinary Medicine, Huazhong Agricultural University, Wuhan 430070, China.
E-mail addresses: zhenfu@uga.edu (Z.F. Fu), penggq@mail.hzau.edu.cn (G. Peng).
[1] Both authors contributed equally to this work.

http://dx.doi.org/10.1016/j.virol.2015.11.018
0042-6822/

infected with MMTV and plays a role in MMTV assembly (Beyer et al., 2013) .

In this study, we demonstrated that P could bind directly to L9 both in vitro and in vivo. This interaction between P and L9 has a biological effect on RABV replication.

Results

Screening of P-interacting cellular partners

To screen cellular proteins that interact with P, His-tagged P was expressed and purified. Using a phage display method, a human brain cDNA library was screened with purified P as the bait. Several P-interacting candidate proteins were identified (Table 1), such as RPL9, KH domain, NEF-E, coiled-coil domain-containing 12, ATP-binding cassette A, splicing factor 45, and proline-rich nuclear receptor coactivator 2. Among the identified cellular factors, we were particularly interested in viral replication-related proteins. Considering the important role of L9 in mouse mammary tumor virus (MMTV) assembly, we decided to focus on investigating the potential role of L9 in RABV replication.

P binds to L9 both in vitro and in vivo

The binding of P to L9 in vitro was determined by GST pull-down assay. The purified GST-tagged L9 (or GST) and His-tagged P were co-incubated with glutathione agarose beads, and the bound proteins were eluted with elution buffer, separated by SDS-PAGE, and subjected to Western blotting with an anti-His antibody. The results indicate that GST-L9 can pull down P (Fig. 1A). To examine whether P interacts with L9 in the context of RABV infection, GST-L9 was immobilized on glutathione agarose beads. Virus-infected or uninfected 293T cell lysates were used in the GST pull-down assay and probed for the presence of P. GST-L9 could pull down P specifically from the RABV-infected cells (Fig. 1B). To further confirm P binding to the L9 protein in vivo, immunoprecipitation analysis was performed. Here, 293T cells were co-transfected with the plasmids pcDNA3.1-P-Fc and pcDNA3.1-L9-V5, expressing Fc-tagged P and V5-tagged L9 protein, respectively. The protein extracts obtained as a result of co-transfection of plasmids were immunoprecipitated with protein A/G agarose and detected by Western blotting with a V5-tag antibody. The results reveal that L9 is co-immunoprecipitated with P (Fig. 1C).

The central domain of P is essential for its binding to L9

The sequence of P required for its binding to L9 was determined using a protein pull-down assay. GST-L9 was generated and immobilized on glutathione agarose beads. His-tagged full-length or truncations of P ($P_{19–297}$, $P_{52–297}$, $P_{82–297}$, $P_{138–297}$, $P_{172–297}$, $P_{1–137}$, $P_{1–180}$, and $P_{1–218}$) were prepared (Fig. 2A) and used in the protein pull-down analysis. The results indicate that GST-L9 can specifically pull down P, and the central domain (residues 138–180) of P is crucial for its binding with L9 (Fig. 2B). To further confirm the binding site, the $P_{\triangle 138–180}$ protein with the central domain (residues 138–180) deleted was constructed and analyzed using the pull-down assay (Fig. 3C). As expected, the $P_{\triangle 138–180}$ protein could not pull down the L9 protein (Fig. 3D).

The N terminal 39 residues of L9 are not involved in the interaction with P

We used a similar strategy to investigate the sequence of L9 required for its binding to P. A full-length His-tagged P was generated and immobilized on nickel-nitrilotriacetic acid agarose beads. The full-length GST-tagged L9 and truncated L9 ($L9_{1–39}$, $L9_{1–61}$, $L9_{1–85}$, $L9_{62–192}$, $L9_{86–192}$, and $L9_{97–192}$) (Fig. 3A) were

Table 1
Phage display-screened cellular factors interacting with the P protein.

No	Name	Size (bp)	Function
1	Ribosomal protein L9	579	60S ribosomal composition, protein translation correction role, pseudogenes
2	Negative-elongation factor E	1143	Participates with RNA polymerase II, role in the negative regulation of translation
3	Coiled coil domain 12	540	Upstream transport along neuronal axons, related to nutrient transport and signal transduction
4	ATP-binding cassette A	4746	Belong to ABC superfamily, is a key mediator of cholesterol and phospholipid efflux to apolipoprotein particles; causes adrenal and brain protein malnutrition
5	KH domain	1038	Transcribed within the nucleic acid-binding protein, responsible for RNA identification
6	Splicing factor 45	1206	Combined with single 3 'AG, exon and intron catalytic reactions and splicing
7	Proline-rich nuclear receptor coactivator 2	420	A new type of nuclear receptor regulatory protein, may be involved in nonsense-mediated mRNA decay

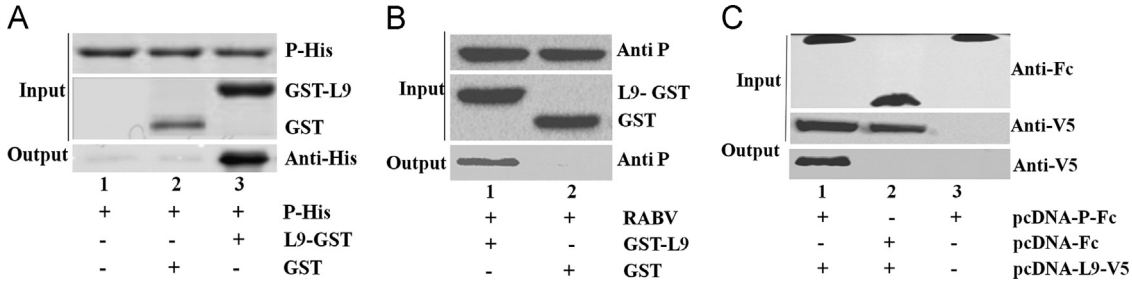

Fig. 1. Identification of the interaction between P and L9 in vivo and vitro. (A) Identification of the protein-protein interactions by GST pull-down in vitro. Purified GST-tagged L9 (or GST) and His-tagged P were co-incubated with glutathione agarose beads. P (top panel) and L9 (middle panel) were detected by SDS-PAGE, and the bound proteins were subjected to Western blotting with an anti-His antibody (bottom panel). Lane 1, P-His protein only; lane 2, P-His protein plus GST; lane 3, P-His protein plus L9-GST. (B) Detection of P and L9 protein interaction in vivo. GST-tagged L9 (or GST) was bound to GST agarose beads. Some of the proteins isolated using the beads were resolved by SDS-PAGE, and the rest were incubated with the 293T cell lysate of RABV-infected cells and detected by Western blotting with an anti-P antibody. Lane 1, RABV-infected cell lysate treated with GST-L9-bound agarose beads; lane 2, RABV-infected cell lysate treated with GST-bound agarose beads. (C) Detection of P and L9 interactions in 293T cells by in vivo immunoprecipitation. 293T cells were co-transfected with pcDNA-P-Fc and pCDNA-L9-V5, immunoprecipitation was performed with protein A/G agarose, and proteins were detected by Western blotting with an anti-V5 antibody. Lane 1, P-Fc protein plus L9-V5; lane 2, Fc protein plus L9-V5; lane 3, P-Fc alone.

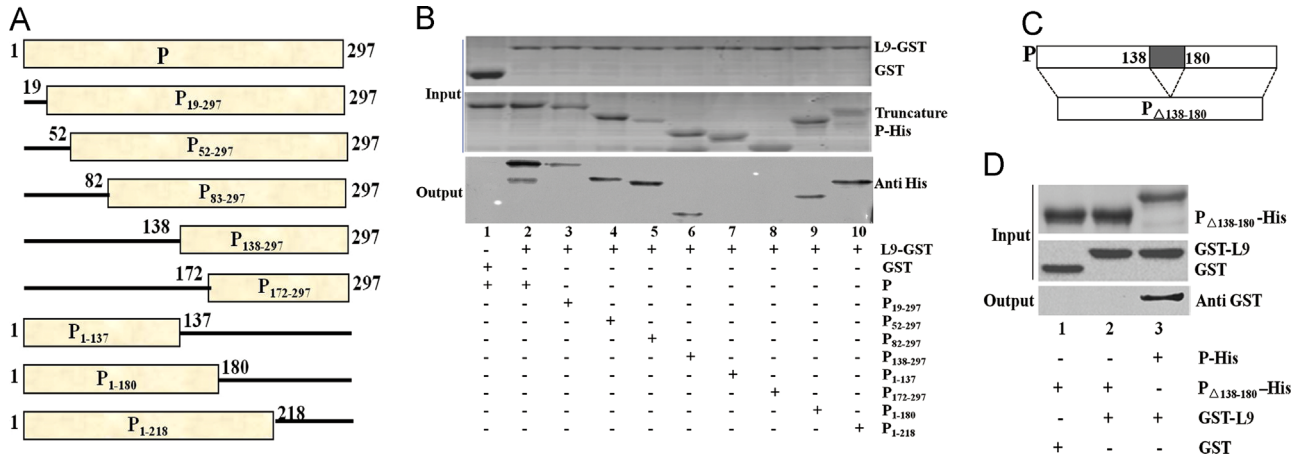

Fig. 2. Identification of the essential domain of P binding with L9 by GST pull-down assay. (A) A schematic representation of P truncation. The numbers indicate the amino acid positions of P. (B) Functional analysis of P binding to L9 by GST pull-down assay. Purified GST-tagged L9 (or GST) and His-tagged truncated P were co-incubated with glutathione agarose beads. L9-GST(or GST) (top panel) and P truncated proteins (middle panel) were detected by SDS-PAGE, and the bound proteins were subjected to Western blotting with an anti-His antibody (bottom panel). Lane 1 represents P plus GST; lanes 2, 3, 4, 5, 6, 7, 8, 9 and 10 represent P, P_{19-297}, P_{52-297}, P_{82-297}, $P_{138-297}$, $P_{172-297}$, P_{1-137}, P_{1-180} and P_{1-218} plus L9, respectively. (C) Schematic representation of P with the deletion of residues 138–180; (D) A further determination of the interaction between $P_{\triangle 138-180}$ and L9 by His-pull-down. Lane 1, GST plus His-tagged $P_{\triangle 138-180}$; lane 2, GST-tagged L9 plus His-tagged $P_{\triangle 138-180}$; lane 3, GST-tagged L9 plus His-tagged P.

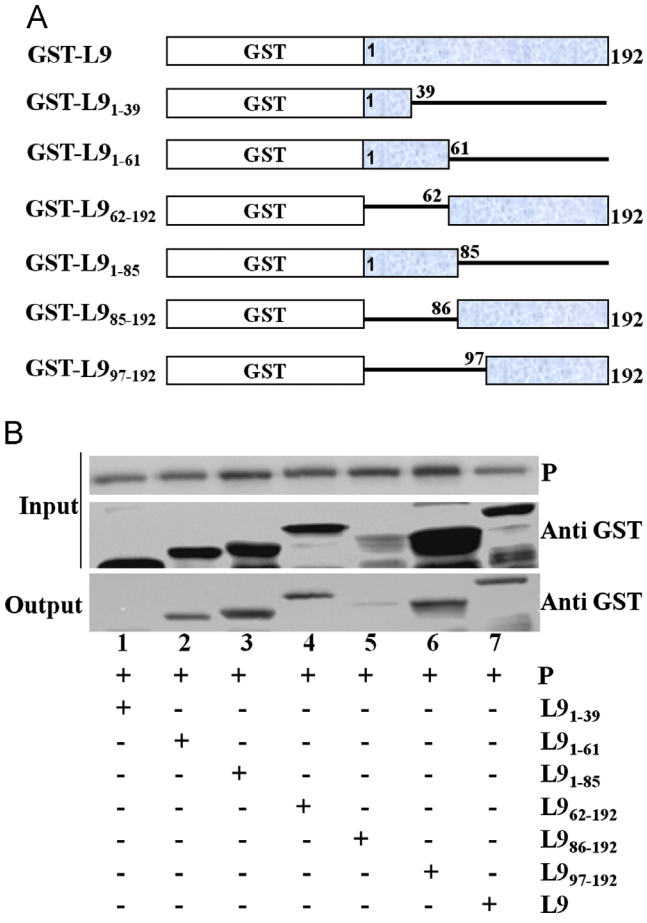

Fig. 3. Identification of the essential domain of L9 protein binding with P by His pull-down assay. (A) A schematic representation of the L9 protein deletions and fusion proteins. The numbers indicate the amino acid positions of the L9 protein. (B) Functional analysis of L9 binding to P by pull-down assay. Purified GST-tagged truncated L9 (or GST) and His-tagged P were co-incubated with His-bound sepharose beads. P was detected by SDS-PAGE (top panel), the bound proteins and L9 truncated proteins were subjected to Western blotting with an anti-GST antibody (middle panel and bottom panel). Lanes 1, 2, 3, 4, 5, 6 and 7 represent $L9_{1-39}$, $L9_{1-61}$, $L9_{1-85}$, $L9_{62-192}$, $L9_{86-192}$, $L9_{97-192}$ and L9 plus P, respectively.

prepared and used in the protein pull-down analysis. As shown in Fig. 3B, P could pull down both the full-length L9 and the C terminus of L9, suggesting that the N terminus of L9 (residues 1–39) is not involved in the interaction with P (Fig. 3B).

P stimulates the translocation of L9 from the nucleus to the cytoplasm

To investigate the cellular localizations of P and L9, 293T cells were transfected with plasmids expressing EGFP-P or DsRed-L9 fusion proteins. The fusion protein localizations in cells were directly observed by LSCM. DsRed-L9 was mainly localized in the nucleus (Fig. 4A), whereas EGFP-P was uniformly distributed in the cytoplasm (Fig. 4B).

The biological interaction between P and L9 was determined by examining the co-localization of the two proteins. The plasmids expressing the EGFP-P or DsRed-L9 fusion proteins were co-transfected into 293T cells. The localizations of the fusion proteins were detected by LSCM. More DsRed-L9 protein was observed in the cytoplasm co-localizing with the EGFP-P rather than distributed in the nucleus (Fig. 4C), indicating that P co-localization with L9 resulted in the translocation of L9 from the nucleus to the cytoplasm. The effects of P on the cellular distribution of L9 were further confirmed in RABV-infected cells. As shown in Fig. 4D, L9 mainly co-localized with P in the cytoplasm of RABV-infected cells.

L9 overexpression reduces RABV replication

Finding that L9 can interact with P in the cytoplasm raised the possibility that L9 could play a role in virus production. To test this idea, 293T cells were infected with rAAV-L9 to overexpress L9 and were subsequently infected with RABV-Rluc. In these cells, RABV replication was decreased significantly. Meanwhile, 293T cells were infected with rAAV-GFP to overexpress GFP and then infected with RABV-Rluc as the control. The luciferase activity in L9-overexpressing cells was reduced nearly 10–20-fold for different doses of RABV-Rluc infection compared with the control (i.e., MOIs of 10^{-1}–10^{-4}) (Fig. 5A). This result was confirmed by Western blot analysis performed from the lysates of these infected cells. P expression in these two cell lines was observed and indicated that

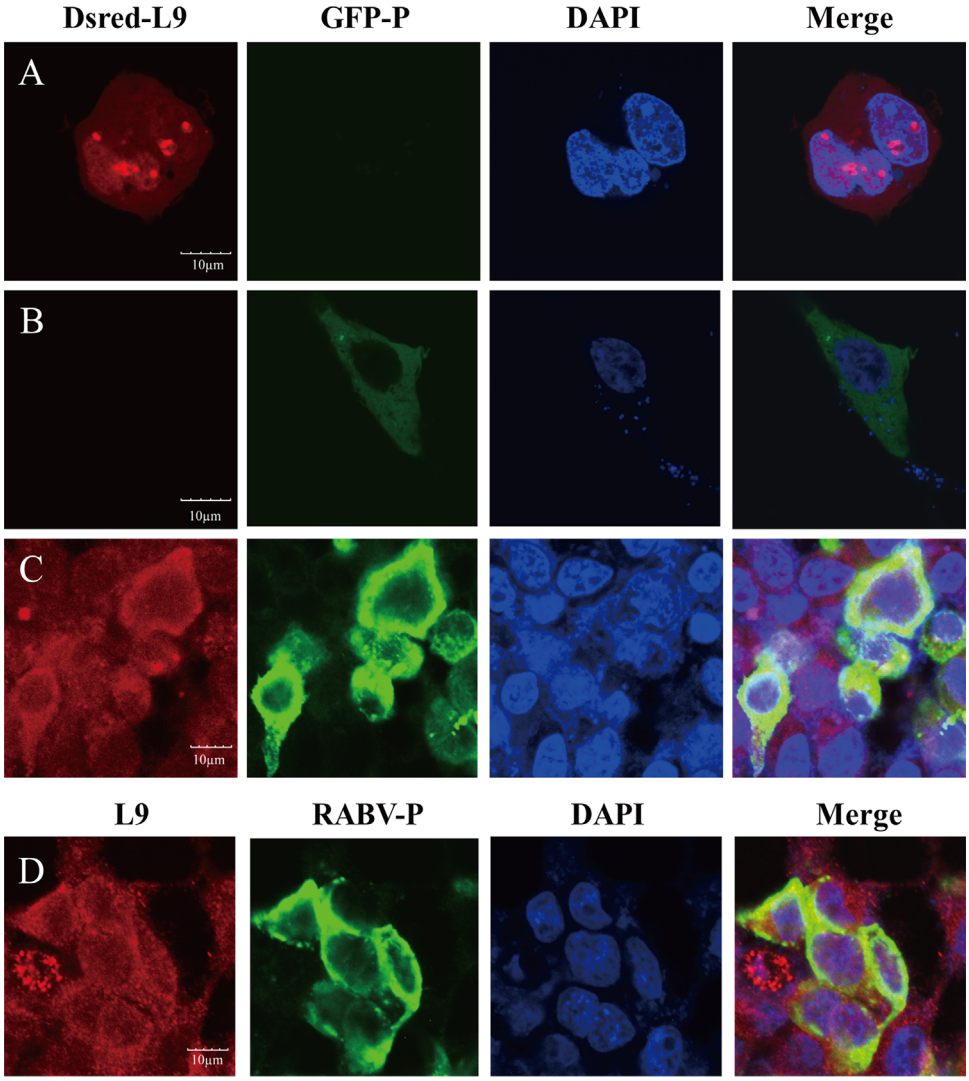

Fig. 4. Identification of the subcellular distribution and colocalization of the L9 and P (A and B). 293T cells were transfected with pDsRed-L9 or pEGFP-P individually. The distributions of the fusion proteins DsRed-L9 (A) and GFP-P (B) were examined using confocal LSCM. (C) pDsRed-L9 and pEGFP-P were cotransfected into 293T cells. The colocalization of the fusion proteins GFP-P with DsRed-L9 was detected using a confocal LSCM. (D) To investigate the colocalization of P and L9 in RABV-infected 293T cells, anti-P and anti-L9 antibodies were used as primary antibodies, and FITC-labeled anti-mouse IgG antibody and tetramethyl rhodamine isothiocyanate-labeled anti-rabbit IgG antibody were used as the respective secondary antibodies. The two proteins were detected using a confocal LSCM. To show the location of the nuclei, the cells were stained with DAPI. Scale bar, 10 μm.

less viral proteins are expressed in L9-overexpressing cells (Fig. 5B). Further, we examined RABV growth curves in SK-N-SH cells to investigate the effect of overexpressing L9 on RABV replication. There was a 10-fold decrease in viral production from 36 to 48 h in the presence of overexpressed L9 (Fig. 5C). To determine whether L9 influence on decreased viral replication was unique to RABV, the growth curves of VSV in rAAV-L9 and rAAV-GFP-infected cells were also determined. As shown in Fig. 5D, there was no significant change in virus production between L9-overexpressing cells and GFP-overexpressing cells at 5, 10, 15, 20, 25 and 30 h. All of the results above indicated that L9 interfered with RABV replication specifically via its binding to P.

The knockdown of L9 expression enhances RABV replication

To further confirm that L9 plays a role in RABV replication, the L9 gene was knocked down using an L9-specific siRNA. Specifically, 293T cells were transfected with an L9-specific siRNA or a scrambled siRNA and were then infected with RABV. The effect of L9-siRNA treatment on L9 expression relative to the β-actin loading controls was evaluated by Western blotting and luciferase assay. The siRNA treatment reduced the L9 expression by approximately 51% compared with the scrambled control siRNA ($P < 0.05$) (Fig. 6A). The virus yield from the cells treated with the L9 siRNA was enhanced 4.84-fold, and P expression was enhanced by approximately 61% (Fig. 6B and C).

The initial transcription of RABV is affected by P-L9 interaction

To investigate which step of the viral cycle is affected by P-L9 interaction, RNA analysis in the presence of cycloheximide was performed by qRT-PCR. The qRT-PCR results show that mRNA copy numbers in L9-overexpressing cells were significantly reduced (31.2–65.4%) compared with the controls treated with or without CHX from 6 to 24 h (Fig. 7A). As a control, the level of VSV N mRNA was unaffected in L9-overexpressing cells treated with or without CHX from 6 to 24 h (Fig. 7B). Overall, our results show that the initial transcription of RABV is affected by P-L9 interaction.

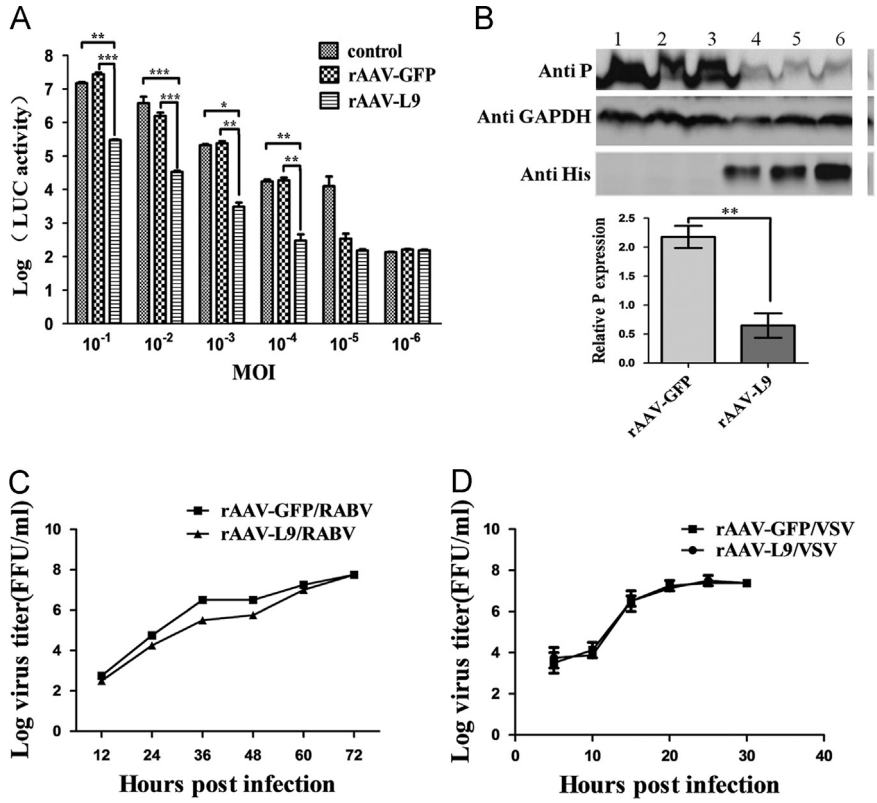

Fig. 5. The effect of L9 overexpression on RABV yield. (A) To investigate the effect of overexpressing L9 on RABV replication, SK-N-SH cells were infected at an MOI of 0.1 with rAAV-L9 and rAAV-GFP. After 12 h, the cells were infected with 10^{-1}, 10^{-2}, 10^{-3}, 10^{-4}, 10^{-5} and 10^{-6} MOI RABV-Rluc for 36 h. Then, the luciferase activities were examined using a single luciferase assay system (Promega), with the error bars representing the means ± standard errors of the mean ($n=5$). One-way ANOVA and Student's *t*-test were performed to compare the treatment groups; *, $P<0.05$, **, $P<0.01$. (B) To investigate the effect of overexpressed L9 on RABV replication, 293T cells were infected at an MOI of 0.1 with rAAV-L9 and rAAV-GFP. After 12 h, the cells were infected with 10^{-1} MOI RABV-Rluc for 48 h. P and His-tagged L9 levels were determined by Western blot using anti-P and anti-His antibodies, respectively. Lanes 1–3, rAAV-GFP plus RABV infection; lanes 4–6, rAAV-L9 plus RABV infection. (C) SK-N-SH cells were infected with rAAV-L9 and rAAV-GFP at an MOI of 0.1. After 24 h, the cells were infected using 0.1 MOI RABV-GFP. Then, the viral titers were detected via a direct immunofluorescent method at 12, 24, 36, 48, 60 and 72 h, and the viral growth curves were generated using GraphPad 5. (D) To prove a specific effect of L9 on RABV, 293T cells were infected with rAAV-L9 and rAAV-GFP. After 12 h, the cells were infected with VSV at an MOI of 0.1. Then, the viral titers were detected via a direct immunofluorescent method at 5, 10, 15, 20, 25 and 30 h. The viral growth curves were generated using GraphPad 5.

Discussion

Rabies remains a public health threat, with more than 59,000 fatalities each year worldwide. P plays important roles in viral replication and transcription by binding to the N and L viral proteins. In addition, P can bind STATs to inhibit IFN production and to evade the innate immunity (Brzozka et al., 2005; Vidy et al., 2005; Wiltzer et al., 2014). P can also interact with LC8, which may be relevant to minus-end-directed axonal transport (Tan et al., 2007). As an essential cofactor of the virus RdRp, P may take part in additional physiological processes (Marschalek et al., 2012). To explore these additional functions of P, we used purified P as the bait to identify its cellular targets using a phage display approach. In our study, we identified 7 cellular factors that may interact with P. One of the candidates, L9, is a component of the 60S ribosome and has a role in protein translation correction (Ulrich Stelzl et al., 2001; Nature Publishing Group). In addition, NEF-E interacts with RNA polymerase II as a negative regulator of translation (Wu et al., 2005), and KH is a nucleic acid-binding protein responsible for the identification of RNA (Valverde et al., 2008).

Previous studies have demonstrated that L9 plays an important role in interacting with the Gag protein of MMTV and translocates the Gag from the cytoplasm to nucleus, influences MMTV assembly . We propose that the interaction between P and L9 may also serve to modulate RABV replication.

In this study, the direct binding of P to L9 was identified using several independent approaches, such as pull-down and co-immunoprecipitation analyses. All of the results were consistent, demonstrating that P interacts directly with L9 both in vivo and in vitro. Amino acids 138–180 of P, which constitute a disordered domain, are important for the interaction with L9, as determined by GST pull-down (Gerard et al., 2009). This domain also overlaps the binding sites between P and the dynein protein LC8 or mitochondrial complex I (Kammouni et al., 2015; Raux et al., 2000). One previous study showed that residues 1–19 of P are responsible for its interaction with the RABV L and that two domains (residues 69–139 and 268–297) are responsible for its interaction with the RABV N (Vidy et al., 2005) . In addition, the C-terminal residues 173–297 of P are responsible for its interaction with STAT1 (Brzozka et al., 2005). These findings are consistent with the multi-functional characteristics of P as a cofactor.

In the present study, we also identified that the N terminal 39 residues of L9 are not involved in the interaction with P. The N-terminal domain (residues 1–84) of L9 is responsible for binding the r-protein in the ribosome, while a larger C-terminal domain (residues 85–192) binds to RNA (23S/28S) (Adamski et al., 1996; Horng et al., 2002). However, it is not yet known if the interaction between P and L9 affects the binding affinity of L9 and RNA. Further studies are needed to investigate this possibility.

The cellular co-location of L9, P and their interactions in mammalian cells were evaluated in this study. The two proteins were over-expressed by transfecting plasmids individually in different cell lines. P localized in the cytoplasm, while L9 was distributed throughout the cell, though predominantly in the

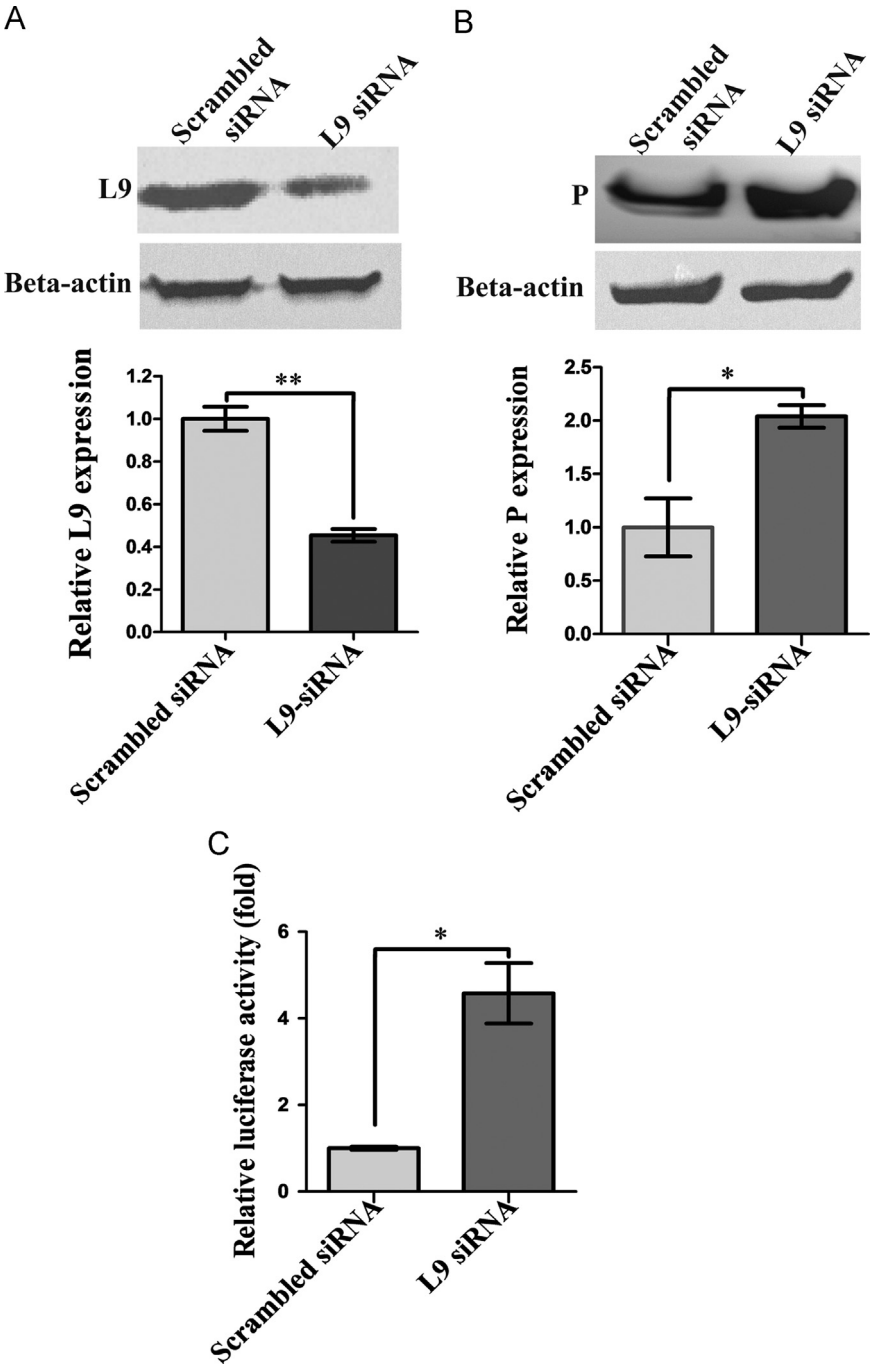

Fig. 6. The effect of L9 depletion on RABV production. 293T cells were infected and treated with L9-specific or scrambled control siRNA, followed by infection with RABV (0.1 MOI). (A) The effect of L9-siRNA treatment on the L9 expression relative to the β-actin loading controls, with the error bars representing the means ± standard deviations ($n=5$). Two-tailed Student's t-tests were performed to compare the treatment groups; *, $P<0.05$. A representative Western blot is shown on the left, indicating a selective reduction in L9 expression. (B) The effect of L9-siRNA treatment on the expression of P relative to the β-actin loading controls. (C) The effect of the L9-siRNA treatment on the RABV yield relative to the scrambled siRNA treatment controls.

nucleolus and nucleus. However, when the two proteins were present in the same cells, P could bind to and recruit L9 to the cytoplasm and promote its reduced distribution in the nucleolus. More interestingly, the same results were obtained using an indirect immunofluorescence assay in RABV-infected 293T cells. L9 distributed in the cytoplasm, co-localizing with P. These results may indicate that P may play a role in the translocation of L9 from the nucleus to the cytoplasm. It has been reported that some viruses hijack host ribosomal proteins to facilitate their own replication (Warner and McIntosh, 2009). For instance, the MMTV Gag protein can interact with the L9 protein and contribute to its assembly (Beyer et al., 2013) . Moreover, overexpression of the ribosomal protein L4 could increase the expression of the MLV Gag-Pol fusion protein (Beyer et al., 2013) . Ribosomal proteins S5 and S9 interact with the hepatitis C virus RNA internal ribosome entry site for optimal translation of viral proteins (Monach et al., 1995). Thus, we propose that RABV replication may be modulated by the interaction between P and L9. Indeed, RABV replication was significantly reduced when the L9 protein was over-expressed, and RABV replication was significantly enhanced when the expression of L9 was knocked down. This effect on RABV replication is specific because such an effect was not observed in cells infected with VSV,

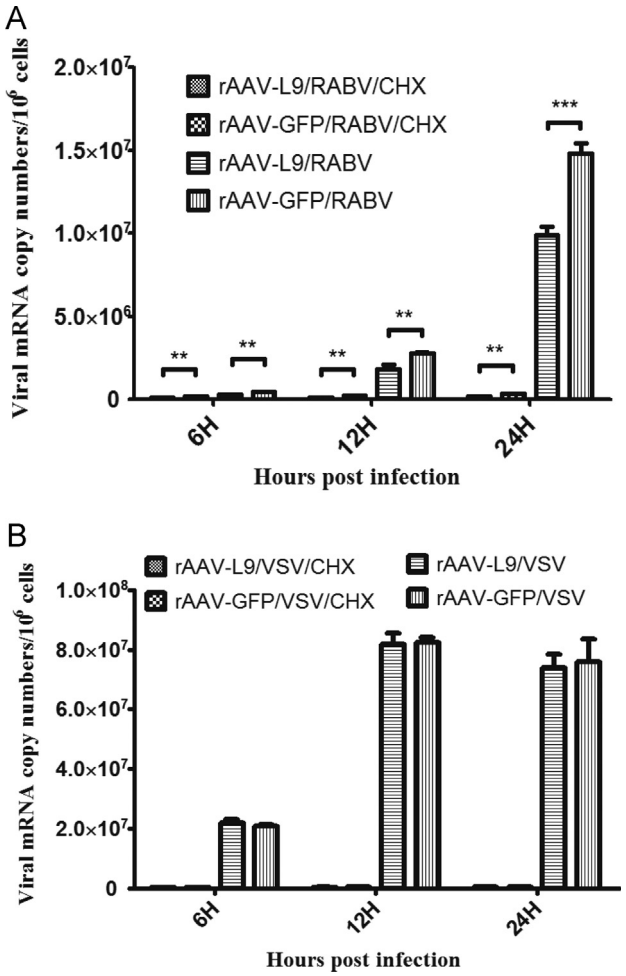

Fig. 7. The effect of L9 overexpression on the initial transcription of RABV. To investigate which step of the viral cycle is affected by P-L9 interaction, 293T cells were infected with rAAV-L9 or rAAV-GFP for 24 h and then infected with RABV or VSV. CHX was added into cells at a final concentration of 100 μg/ml 1 h before virus infection. At 6, 12, and 24 h after virus infection, cells were harvested and subjected to quantitative real-time PCR (qRT-PCR). (A) The effect of overexpressed L9 on RABV mRNA production was determined by qRT-PCR when the cells were treated with or without CHX at 6, 12 and 24 h. Two-tailed Student's *t*-tests were performed to compare the treatment groups; **, $P<0.01$, ***, $P<0.001$. (B) As a control, the effect of overexpressed L9 on VSV mRNA production was determined by qRT-PCR when the cells treated with or without CHX at 6, 12 and 24 h. Two-tailed Student's t-tests were performed to compare the treatment groups.

a virus phylogenetically similar to RABV (Gerard et al., 2009). P plays multiple roles during the viral replication cycle (Gerard et al., 2009). In the initial stages of viral infection, P and N form a complex, which keeps N in a soluble and monomeric form and prevents cellular RNA from binding N, thus preserving the N for specifically encapsidating the viral RNA (Gerard et al., 2009; Mavrakis et al., 2003). In addition, P acts as a cofactor of the L protein in both the viral transcription and replication processes (Qanungo et al., 2004; Wang et al., 2014). L performs all of the enzymatic activities but is unable to bind to viral nucleocapsids. P binds to both nucleocapsids and L, which allows the association of the polymerase with its template (Mavrakis et al., 2003). Thus, L9 may disturb the function of P as a viral noncatalytic cofactor and may thereby modulate RABV replication.

Previous studies have shown that host molecules can modulate the transcriptional activity of a viral polymerase. For example, heat shock protein 72 can interact with the nucleoprotein of measles viruses (Zhang et al., 2005), enhance viral polymerase efficiency, and subsequently increase mortality in mice (Carsillo et al., 2006). The dynein light chain (LC8) was shown to interact with RABV P (Raux et al., 2000), and involved in primary viral transcription (Tan et al., 2007). Likewise, it is possible that L9 may also regulate the efficiency of the RABV viral polymerase complex in a mechanism that has yet to be defined.

.Based on our results, we propose a model of the effect of L9 on RABV replication. In the initial stage of RABV infection, L9 interacts with the P protein and may disturb the function of P as a viral noncatalytic cofactor, decreasing but not completely blocking RABV transcription. As the infection progresses, more and more P protein is expressed, while the amount of L9 is not significantly altered. Then, superfluous P protein can participate in viral replication at a later stage. It partially explains why RABV infectious cycle is very slow when compared with that of VSV, which helps RABV to escape the immune responses. In summary, we demonstrate that P can bind directly to L9 and can translocate L9 from the nucleus to the cytoplasm, which inhibit the initial stages of RABV transcription. This study serves as a reference for future studies aiming to understand the function of P and its potential as a new drug target.

Materials and methods

Cell culture and virus propagation

HEK-293T and human neuroblastoma cells (SK-N-SH) cells were maintained in RPMI 1640 and Minimum essential medium (MEM) containing 10% heat-inactivated fetal bovine serum (FBS). In general, the adherent cells were infected with RABV or vesicular stomatitis virus (VSV) at a multiplicity of infection (MOI) of 0.1 in 1640 or DMEM containing 2% FBS and were then incubated for 2 to 4 days. The RABV (SAD-L16 strain), RABV-Rluc (recombinant SAD-L16 strain expressing Renilla luciferase reporter) and RABV-GFP strains (recombinant SAD-L16 expressing EGFP) were stored at −80 °C, and VSV-GFP (recombinant VSV expressing GFP) was a gift from Dr. Mingzhou Chen of Wuhan University.

Plasmid construction

P gene of RABV (SAD-L16) was amplified from P helper plasmid used in the reverse genetic system (Zhao et al., 2009). The PCR product was cloned into pET-42b with a C-terminal His_6 tag to yield the plasmid pET42b-P. P-truncated variants used in this study were designed according to previous studies (Blondel et al., 2002) and cloned into pET-42b with a C-terminal His_6 tag to yield the plasmids pET42b-P_{19-297}, pET42b-P_{52-297}, pET42b-P_{82-297}, pET42b-$P_{138-297}$, pET42b-$P_{172-297}$, pET42b-P_{1-137}, pET42b-P_{1-180}, and pET42b-P_{1-218}. To generate pEGFP-P, P gene was amplified from PET42b-P, and the PCR product then was cloned into pEGFP-N1. To yield the plasmids pcDNA3.1-P and pcDNA3.1-P-Fc, P gene was amplified from PET42b-P, and the PCR products were cloned into pcDNA3.1 and pcDNA3.1-Fc. To generate pET42b-$P_{\triangle 138-180}$, the $P_{\triangle 180-297}$ gene with homologous arms was amplified from pET42b-P, and the PCR product was recombined into PET42b-P_{1-137}.

The L9 gene was amplified from a selected T7 phage cDNA bank by PCR and then cloned into the pGEX-KG vector to yield the plasmid pGEX-KG-L9, which could express the fusion protein GST-L9. All of the L9-truncated variants, pGEX-KG-$L9_{1-39}$, pGEX-KG-$L9_{1-61}$, pGEX-KG-$L9_{1-85}$, pGEX-KG-$L9_{62-192}$, pGEX-KG-$L9_{86-192}$, and pGEX-KG-$L9_{97-192}$, were designed according to previous studies (Beyer et al., 2013; Hoffman et al., 1994) and constructed on the basis of plasmid pGEX-KG-L9. To generate pDsRed-L9, pcDNA3.1-L9-V5, and pAAV-CMV-L9, the L9 gene was amplified from pGEX-KG-L9 and then inserted into pDsRed-N1, pcDNA3.1-V5 and pAAV-CMV, respectively.

Protein expression and purification

P or its mutants were expressed and purified as described previously (Peng et al., 2008). Briefly, the plasmid pET42b-P, fused in frame with a C-terminal His_6 tag, was transformed into *Escherichia coli* BL21, and protein expression was induced with 0.5 mM isopropyl β-D-1-thiogalactopyranoside (IPTG) for 3 h at 37 °C. After the incubation, cells were centrifuged and lysed followed by centrifuging for 45 min at 8500 rpm and 4 °C. The protein in the supernatant was purified sequentially by nickel-nitrilotriacetic acid (GE Healthcare, Uppsala, Sweden) and gel-filtration columns. All of the other truncations of P were expressed and purified using the same approach. The L9 and L9-truncated fragments were fused with an N-terminal glutathione S-transferase (GST) tag and expressed using the same strategy as P. A GST Trap HP column (GE Healthcare, Uppsala, Sweden) and a Superdex 200 pg gel filtration column were used for L9 purification.

T7 select biopanning

A premade human brain cDNA library (No. 70550-3, Novagen) was screened with the T7 Select biopanning kit (Novagen) according to the manufacturer's instructions. The purified P was used as the bait. After five rounds of selection, 236 randomly selected clones were sequenced and blasted with known sequences using the online program (http://www.ncbi.nlm.nih.gov/BLAST).

Protein pull-down assays

The purified GST-tagged L9 (or GST) and His-tagged P (or His-tagged P-truncated proteins) were co-incubated with glutathione agarose beads. After washing, the bound proteins were eluted with elution buffer, separated by sodium dodecyl sulfate gel electrophoresis (SDS-PAGE), and subjected to Western blotting with a mouse anti-His monoclonal antibody (1:5000, Boster, Wuhan, Hubei, China) and a horseradish peroxidase (HRP)-conjugated goat anti-mouse IgG antibody (1:5000, Proteintech, Wuhan, Hubei, China).

To examine whether P interacts with the L9 in the context of RABV infection, the purified GST-tagged L9 and RABV-infected 293T cell lysate were co-incubated with glutathione agarose beads. The bound proteins were separated by SDS-PAGE and detected by Western blotting with HRP-conjugated anti-P mouse monoclonal antibodies (1:8000).

To identify the essential domain of L9 for its interaction with P, the purified His-tagged P and L9 truncated proteins were co-incubated with nickel-nitrilotriacetic acid agarose beads. The bound proteins were detected by SDS-PAGE and Western blotting with rabbit anti-GST polyclonal antibodies (1:5000, Boster, Wuhan, Hubei, China) and goat anti-rabbit HRP-conjugated IgG antibody (1:5000, Proteintech, Wuhan, Hubei, China). All the Western blottings were developed using a chemiluminescence reagent (ECL, Beyotime, Shanghai, China) and visualized with the G:Box Chemi XT4 (Syngene UK).

Co-immunoprecipitation assay

The 293T cells were co-transfected with pcDNA3.1-L9-V5 and pcDNA3.1-P-Fc, which express a V5-tagged L9 and an Fc-tagged P, respectively. After 48 h, the cells were lysed and centrifuged; the supernatants were incubated with protein A/G-agarose beads (Santa Cruz Biotechnology). After three washes with radioimmunoprecipitation assay (RIPA) buffer, the proteins bound to the beads were separated by SDS-PAGE. Then, Western blotting analysis was performed with a mouse V5 tag antibody (1:5000, Proteintech, Wuhan, Hubei, China) and an HRP-conjugated goat anti-mouse IgG antibody.

Laser-scanning confocal microscopy analysis

The recombinant plasmids pDsRed-L9 and pEGFP-P were co-transfected into 293T cells that were cultured on cover slips in a 24-well plate. After 30 h, the cells were fixed with 4% paraformaldehyde for 15 min and then washed three times with PBS. The nuclei were counterstained with 4′,6-diamidino-2-phenylindole (DAPI) for 10 min, and the slides were washed three times with PBS. The fluorescence was detected using a Laser-scanning confocal microscope (LSCM, FV1000 Fluo View; Olympus). Meanwhile, pDsRed-L9 and pEGFP-P were individually transfected into 293T cells to verify the locations of L9 and P. To verify the locations of P and endogenous L9, 293T cells were infected with RABV for 30 h, fixed with 4% paraformaldehyde and blocked with 5% skim milk. The cells were incubated with a mouse anti-P monoclonal antibody in PBS containing 5% skim milk and a rabbit anti-L9 polyclonal antibody (1:300, Santa Cruz Biotechnology, Inc.) for 2 h at room temperature (RT) and then washed three times with PBST. The cells were incubated with a fluorescein isothiocyanate (FITC)-conjugated goat anti-mouse IgG antibody (1:300, Invitrogen, Carlsbad, CA, USA) and a tetramethyl rhodamine isothiocyanate-conjugated goat anti-rabbit IgG antibody (1:300, Invitrogen, Carlsbad, CA, USA) for 1 h. The fluorescence was detected using LSCM.

L9 overexpression and virus yield assays

The 293T cells were co-transfected with the pAAV-CMV-L9 (or pAAV-CMV-GFP), pHelper, and pAAV-DJ plasmids (Moshiri et al., 2014). After 48 h, the cells were pelleted by centrifugation, and rAAV-L9 and rAAV-GFP were prepared by freezing and thawing. To investigate the effect of L9 overexpression on RABV replication, SK-N-SH cells were infected with rAAV-L9 or rAAV-GFP at an MOI of 0.1. After 24 h, the cells were infected with RABV expressing the Renilla luciferase reporter at 10^{-1}–10^{-6} MOI for 36 h. Then, the luciferase activities were detected using a single luciferase assay system (Promega), and the results were analyzed by one-way ANOAV using GraphPad Prism 5 (GraphPad Software, Inc. San Diego, California, USA).

SK-N-SH cells were infected with rAAV-L9 or rAAV-GFP at an MOI of 0.1. After 24 h, the cells were infected with RABV-GFP at 0.1 MOI. Then, the viral titers of RABV were detected using a direct immunofluorescence assay at 12, 24, 36, 48, 60 and 72 h, and the viral growth curves were generated using GraphPad Prism 5. To investigate whether the effect of L9 on viral replication is specific for RABV, VSV-GFP was incubated at 0.1 MOI with 293T cells previously infected with rAAV-L9 or rAAV-GFP. Then, the viral titers of VSV were detected using a direct immunofluorescence assay at 5, 10, 15, 20, 25 and 30 h, and the viral growth curves were generated using GraphPad Prism 5.

L9 siRNA-mediated knockdown and virus yield assays

For these assays, 293T cells were seeded in 35-mm dishes at a density of 0.25×10^6 cells/dish and then transfected with L9 siRNA or scrambled control siRNA (GenePharma, Shanghai, China) using Lipofectamine 2000 according to the manufacturer's instructions. After 12 h, the cells were infected at an MOI of 0.1 with RABV-Rluc. After 48 h, the luciferase activities were detected. Normalized amounts were analyzed by Western blotting for L9 and P expression. Each experiment was replicated five times, and the statistical analyses were performed using two-tailed Student's *t*-tests in GraphPad Prism 5.

Treatment of infected cells with Cycloheximide (CHX)

293T cells were infected with rAAV-L9 or rAAV-GFP for 24 h and then infected with RABV or VSV. CHX was purchased from Sigma (St. Louis, Mo.) and added into cells at a final concentration of 100 μg/ml 1 h before infection with RABV or VSV as described previously (Boudinot et al., 2001). At 6, 12, and 24 h after virus infection, cells were harvested and subjected to quantitative real-time PCR (qRT-PCR).

qRT-PCR

The absolute quantification of mRNA was performed as described previously (Yang et al., 2015). Briefly, total RNA were extracted from cells using the RNeasy kit from Qiagen. The cDNA of viral mRNA was synthesized by AMV reverse transcriptase XL (Takara) following the manufacturer's instructions using RABV gene-specific primer RABV-NR (TCATCTGCCAGTGCTACGTC) and VSV gene-specific primer VSV-NR (AGTAGATACAAAGGCAACCA), respectively. qRT-PCR was then performed using primers RABV-NF (GAGGAATTCTTCGGGAAAGG) and RABV-NR, or VSV-NF (GAATAAACATCGGGAAAGCA) and VSV-NR, respectively. A standard curve was generated from serially diluted RNA in vitro transcribed from a plasmid expressing RABV N and VSV N and the copy numbers of RABV mRNA and VSV mRNA were normalized to 1 μg of total RNA. The statistical analyses were performed using two-tailed Student's *t*-tests in GraphPad Prism 5.

Acknowledgments

This work was supported by the National Natural Science Foundation of China (Grant nos. 31330078 and 31372440), the Huazhong Agricultural University Scientific & Technological Self-innovation Foundation (Program nos. 2012RC008 and 2013PY031), and the Doctoral Fund of the Ministry of Education of China (Grant no. 20130146120004) and was supported by the Natural Science Foundation of Hubei Province of China (Grant no. 2013CFB191).

References

Adamski, F.M., Atkins, J.F., Gesteland, R.F., 1996. Ribosomal protein L9 interactions with 23 S rRNA: the use of a translational bypass assay to study the effect of amino acid substitutions. J. Mol. Biol. 261, 357–371.
Beyer, A.R., Bann, D.V., Rice, B., Pultz, I.S., Kane, M., Goff, S.P., Golovkina, T.V., Parent, L.J., 2013. Nucleolar trafficking of the mouse mammary tumor virus gag protein induced by interaction with ribosomal protein L9. J. Virol. 87, 1069–1082.
Blondel, D., Regad, T., Poisson, N., Pavie, B., Harper, F., Pandolfi, P.P., De, H., Chelbi-Alix, M.K., 2002. Rabies virus P and small P products interact directly with PML and reorganize PML nuclear bodies. Oncogene 21, 7957–7970.
Boudinot, P., Salhi, S., Blanco, M., Benmansour, A., 2001. Viral haemorrhagic septicaemia virus induces vig-2, a new interferon-responsive gene in rainbow trout. Fish Shellfish Immunol. 11, 383–397.
Brzozka, K., Finke, S., Conzelmann, K.K., 2005. Identification of the rabies virus alpha/beta interferon antagonist: phosphoprotein P interferes with phosphorylation of interferon regulatory factor 3. J. Virol. 79, 7673–7681.
Carsillo, T., Traylor, Z., Choi, C., Niewiesk, S., Oglesbee, M., 2006. hsp72, a host determinant of measles virus neurovirulence. J. Virol. 80, 11031–11039.
Chenik, M., Chebli, K., Gaudin, Y., Blondel, D., 1994. In vivo interaction of rabies virus phosphoprotein (P) and nucleoprotein (N): existence of two N-binding sites on P protein. J. Gen. Virol. 75, 2889–2896.
Chenik, M., Schnell, M., Conzelmann, K.K., Blondel, D., 1998. Mapping the interacting domains between the rabies virus polymerase and phosphoprotein. J. Virol. 72, 1925–1930.
Moshiri, Farzaneh, Callegari, Elisa, D'Abundo, Lucilla, Corrà, Fabio, Lupini, Laura, Sabbioni, Silvia, Negrini, Massimo, 2014. Inhibiting the oncogenic mir-221 by microRNA sponge: toward microRNA-based therapeutics for hepatocellular carcinoma. Gastroenterol. Hepatol. Bed Bench 7, 12.
Fu, Z.F., Zheng, Y., Wunner, W.H., Koprowski, H., Dietzschold, B., 1994. Both the N- and the C-terminal domains of the nominal phosphoprotein of rabies virus are involved in binding to the nucleoprotein. Virology 200, 590–597.
Gerard, F.C., Ribeiro Ede Jr., A., Leyrat, C., Ivanov, I., Blondel, D., Longhi, S., Ruigrok, R. W., Jamin, M., 2009. Modular organization of rabies virus phosphoprotein. J. Mol. Biol. 388, 978–996.
Hoffman, D.W., Davies, C., Gerchman, S.E., Kycia, J.H., Porter, S.J., White, S.W., Ramakrishnan, V., 1994. Crystal structure of prokaryotic ribosomal protein L9: a bi-lobed RNA-binding protein. EMBO J. 13, 205–212.
Horng, J.C., Moroz, V., Rigotti, D.J., Fairman, R., Raleigh, D.P., 2002. Characterization of large peptide fragments derived from the N-terminal domain of the ribosomal protein L9: definition of the minimum folding motif and characterization of local electrostatic interactions. Biochemistry 41, 13360–13369.
Jackson, A.C., 2002. Update on rabies. Curr. Opin. Neurol. 15, 327–331.
Jacob, Y., Real, E., Tordo, N., 2001. Functional interaction map of lyssavirus phosphoprotein: identification of the minimal transcription domains. J. Virol. 75, 9613–9622.
Kammouni, W., Wood, H., Saleh, A., Appolinario, C.M., Fernyhough, P., Jackson, A.C., 2015. Rabies virus phosphoprotein interacts with mitochondrial Complex I and induces mitochondrial dysfunction and oxidative stress. J. Neurovirol. 21, 370–382.
Marschalek, A., Drechsel, L., Conzelmann, K.K., 2012. The importance of being short: the role of rabies virus phosphoprotein isoforms assessed by differential IRES translation initiation. Eur. J. Cell. Biol. 91, 17–23.
Mavrakis, M., Iseni, F., Mazza, C., Schoehn, G., Ebel, C., Gentzel, M., Franz, T., Ruigrok, R.W., 2003. Isolation and characterisation of the rabies virus N degrees-P complex produced in insect cells. Virology 305, 406–414.
Mavrakis, M., McCarthy, A.A., Roche, S., Blondel, D., Ruigrok, R.W., 2004. Structure and function of the C-terminal domain of the polymerase cofactor of rabies virus. J. Mol. Biol. 343, 819–831.
Mavrakis, M., Mehouas, S., Real, E., Iseni, F., Blondel, D., Tordo, N., Ruigrok, R.W., 2006. Rabies virus chaperone: identification of the phosphoprotein peptide that keeps nucleoprotein soluble and free from non-specific RNA. Virology 349, 422–429.
McCarthy, M., 2015. Rabies kills 59,000 people worldwide each year, study estimates. BMJ 350, h2189.
Mebatsion, T., 2001. Extensive attenuation of rabies virus by simultaneously modifying the dynein light chain binding site in the P protein and replacing Arg333 in the G protein. J. Virol. 75, 11496–11502.
Monach, P.A., Meredith, S.C., Siegel, C.T., Schreiber, H., 1995. A unique tumor antigen produced by a single amino acid substitution. Immunity 2, 45–59.
Pasdeloup, D., Poisson, N., Raux, H., Gaudin, Y., Ruigrok, R.W., Blondel, D., 2005. Nucleocytoplasmic shuttling of the rabies virus P protein requires a nuclear localization signal and a CRM1-dependent nuclear export signal. Virology 334, 284–293.
Peng, G., Yan, Y., Zhu, C., Wang, S., Yan, X., Lu, L., Li, W., Hu, J., Wei, W., Mu, Y., Chen, Y., Feng, Y., Gong, R., Wu, K., Zhang, F., Zhang, X., Zhu, Y., Wu, J., 2008. Borna disease virus P protein affects neural transmission through interactions with gamma-aminobutyric acid receptor-associated protein. J. Virol. 82, 12487–12497.
Qanungo, K.R., Shaji, D., Mathur, M., Banerjee, A.K., 2004. Two RNA polymerase complexes from vesicular stomatitis virus-infected cells that carry out transcription and replication of genome RNA. P Natl. Acad. Sci. USA 101, 5952–5957.
Raux, H., Flamand, A., Blondel, D., 2000. Interaction of the rabies virus P protein with the LC8 dynein light chain. J. Virol. 74, 10212–10216.
Ray, N.B., Ewalt, L.C., Lodmell, D.L., 1995. Rabies virus replication in primary murine bone marrow macrophages and in human and murine macrophage-like cell lines: implications for viral persistence. J. Virol. 69, 764–772.
Tan, G.S., Preuss, M.A., Williams, J.C., Schnell, M.J., 2007. The dynein light chain 8 binding motif of rabies virus phosphoprotein promotes efficient viral transcription. Proc. Natl. Acad. Sci. USA 104, 7229–7234.
Ulrich Stelzl, S.C., Nierhaus, Knud H., Wittmann-Liebold, Brigitte, 2001. Ribosomal proteins: role in ribosomal functions. In: Nature Publishing Group (Ed.), Encyclopedia of Life Sciences, 12 ed. Nature Publishing Group, United Kingdom, p. 12.
Valverde, R., Edwards, L., Regan, L., 2008. Structure and function of KH domains. FEBS J. 275, 2712–2726.
Vidy, A., Chelbi-Alix, M., Blondel, D., 2005. Rabies virus P protein interacts with STAT1 and inhibits interferon signal transduction pathways. J. Virol. 79, 14411–14420.
Wang, F.X., Zhang, S.Q., Zhu, H.W., Yang, Y., Sun, N., Tan, B., Li, Z.G., Cheng, S.P., Fu, Z. F., Wen, Y.J., 2014. Recombinant rabies virus expressing the H protein of canine distemper virus protects dogs from the lethal distemper challenge. Vet. Microbiol. 174, 362–371.
Warner, J.R., McIntosh, K.B., 2009. How common are extraribosomal functions of ribosomal proteins? Mol. Cell 34, 3–11.
Wiltzer, L., Okada, K., Yamaoka, S., Larrous, F., Kuusisto, H.V., Sugiyama, M., Blondel, D., Bourhy, H., Jans, D.A., Ito, N., Moseley, G.W., 2014. Interaction of rabies virus P-protein with STAT proteins is critical to lethal rabies disease. J. Infect. Dis. 209, 1744–1753.
Wool, I.G., Chan, Y.L., Gluck, A., 1995. Structure and evolution of mammalian ribosomal proteins. Biochem. Cell Biol. (Biochim. Biol. Cell.) 73, 933–947.
Wu, C.H., Lee, C., Fan, R., Smith, M.J., Yamaguchi, Y., Handa, H., Gilmour, D.S., 2005. Molecular characterization of Drosophila NELF. Nucleic Acids Res. 33, 1269–1279.
Yang, Y., Huang, Y., Gnanadurai, C.W., Cao, S., Liu, X., Cui, M., Fu, Z.F., 2015. The inability of wild-type rabies virus to activate dendritic cells is dependent on the glycoprotein and correlates with its low level of the de novo-synthesized leader RNA. J. Virol. 89, 2157–2169.
Zhang, X., Bourhis, J.M., Longhi, S., Carsillo, T., Buccellato, M., Morin, B., Canard, B., Oglesbee, M., 2005. Hsp72 recognizes a P binding motif in the measles virus N protein C-terminus. Virology 337, 162–174.
Zhao, L., Toriumi, H., Kuang, Y., Chen, H.C., Fu, Z.F., 2009. The roles of chemokines in rabies virus infection: overexpression may not always be beneficial. J. Virol. 83, 11808–11818.